

# TOWARDS MORE RESILIENT SMART CITIES: MT-InSAR MONITORING OF URBAN INFRASTRUCTURE USING MACHINE LEARNING TECHNIQUES

I. Rodríguez-Antuñaño<sup>1</sup>\*, J. Martínez-Sánchez<sup>1</sup>, S. Lagüela-López<sup>2</sup>, B. Riveiro<sup>1</sup>

<sup>1</sup> CINTECX, Universidade de Vigo, GeoTECH Group, Campus Universitario de Vigo, As Lagoas, Marcosende, 36310 Vigo, Spain - (ignacio.rodriguez.antunano, joaquin.martinez, belenriveiro)@uvigo.es

<sup>2</sup> Cartographic and Terrain Engineering, Universidad de Salamanca, Calle Hornos Caleros 50, 05003 Ávila, Spain - sulaguela@usal.es

## Commission IV, WG IV/9

**KEY WORDS:** MT-InSAR, machine learning, infrastructure monitoring, predictive monitoring, smart city, resilient urbanism, remote sensing, O Marisqueño Festival pier Collapse.

### ABSTRACT:

Global climate change makes the maintenance and resilience of cities one of the greatest challenges facing civilization. Constant monitoring is essential work to determine if the city and its infrastructure are well preserved. This monitoring has become increasingly simple and affordable, thanks to the advancement of technology, so the current trend is to systematically monitor the entire city (this concept is the paradigm of the smart city). There are several methods for infrastructure monitoring including GPS, mobile-mapping, video-surveillance, etc. However, this type of method has a series of disadvantages, such as the impossibility of obtaining large-scale data or the unavailability of information of the previous, current or after state that an event has occurred in the study-area. This can be solved with monitoring based on satellite images, since these have historical and constant coverage over time, with good resolution to identify urban structures and cover large study areas. The use of satellite radar images through MT-InSAR is booming because it is a powerful remote sensing technique capable of detecting displacements on the earth's surface. This technique can be combined with Machine-Learning to perform predictive analysis in urban environments and detect infrastructure failures. This predictive monitoring capable of anticipating risks is one of the objectives of the new urbanism. For this reason, this work analyzes the collapse of a pier, which occurred in Vigo, a city in NW Spain, through radar satellite images (Sentinel-1), MT-InSAR and Machine-Learning. The result is the possibility of anticipating structural failures thanks to the predictive monitoring.

## 1. INTRODUCTION

### 1.1 From the city to the predictive infrastructure monitoring via remote sensing to achieve the smart city

Currently, there are great efforts made by researchers, political authorities, companies, and urban-planners, to address the problems that global climate change can cause in cities, since a large part of the world's population is concentrated into them. As a solution to this problem, the concept of Smart City appears. Smart City considers that a wide range of urban challenges can be addressed by the Information and Communication Technology, ICT (Anthopoulos, 2015) through the constant monitoring of the city. Even though such monitoring supports the response to multiple problems in an efficient manner, at present a new approach to urbanism is beginning to settle, not focused on solving problems but rather on anticipating problems (Sharifi & Yamagata, 2014).

This resilient urban planning capable of adapting to adverse situations is possible thanks to great technological advances through artificial intelligence subject to the availability of data. In this sense, the availability of free and systematic satellite data is boosting a great revolution in the monitoring of cities and their infrastructures.

There are mainly 2 classes of satellite that can fulfil the objective of monitoring infrastructures via remote sensing:

- Optical Satellites.
- Radar Satellites.

Optical satellite images, despite being visually easier to interpret, are commonly the least used due to their great disadvantages compared to radar images:

- Signals from radar satellites can pass through clouds and therefore can obtain images of the earth's surface covered by clouds and the optical cannot.
- Radar satellites obtain data also in the dark of night and the optical cannot.

Also, based on satellite radar images, various techniques have been developed to be able to extract displacement information (Crosetto et al., 2016; González, 2010; Xue et al., 2020). One of the most used techniques is Multi-temporal Interferometric Synthetic Aperture Radar (MT-InSAR).

MT-InSAR consists of several radar satellites images (Slaves) of different dates compared against a chosen reference image (Master). This comparison produces interferograms, which can be treated later by different programs to obtain displacements

\* Corresponding author

maps (Xue et al., 2020) (in this study, the StaMPS program is chosen, as it is open).

The displacements maps consist of data points with the displacements that have been captured on each of the dates of the comparison images, in addition to including their coordinates.

In this work, since the analysis is in an urban environment and the StaMPS program is the chosen, the method used in the MT-InSAR technique must be PSI (Persistent Scatterer Interferometry). This method consists of identifying pixels through the spatial correlation of the phase (it only uses those with stable phase through the time series). To do this, the method requires the spacing between the spatial and temporal baselines to be reduced for this analysis to be effective. This allows the method to perform an evaluation of the differences in the interferometric phase time in order to obtain the information points with potential to be selected and that must be consistent over time; these selected information points are called Permanent Scatterer (PS) (A. J. Hooper, 2008; Juan Gabriel Arroyo Parras & Antonio Miguel Ruiz Armenteros, 2017).

There are numerous and different types of radar images on the market, but currently only Sentinel-1 images are free and for any type of user, for that reason they are chosen in this work (this facilitates the reproduction of the proposed methodology for other cases of study).

The European Space Agency (ESA) developed a series of next-generation Earth observation missions including Sentinel-1 (<https://sentinels.copernicus.eu/web/sentinel/missions/sentinel-1>), which consists of radar images. These images present a series of advantages for infrastructure monitoring, such as: constant availability every 6 days, the spatial resolution is ~ 20 m and 250km swath with a stable acquisition geometry (Cian et al., 2019). The following table summarizes its main characteristics (Table 1):

Launched	Unit A: 2013/ unit B: 2016
Lifespan	Operational: 7 years / consumables: 12 years
Orbit	Sun-synchronous, near-polar, circular orbit
Instrument	C-band SAR
Coverage	Global
Revisit	12 days (6 days for A- and B-units)
Spatial resolution/ swath width	Strip map mode: 5 × 5m/80 km Interferometric wide-swath mode: 5 × 20m/250 km (standard mode) Extra-wide-swath mode: 20 × 40 m/400 km Wave mode: 5 × 5m/20 × 20 km
Centre frequency:	5.405 GHz
Radiometric accuracy	1 dB (3σ)
Polarisation	VV+VH, HH+HV, HH, VV
Incidence angle:	20° - 45°
Mission Objectives	Land monitoring of forests, water, soil and agriculture Emergency mapping support in the event of natural disasters Marine monitoring of the maritime

environment Sea ice observations and iceberg monitoring Production of high-resolution ice charts Forecasting ice conditions at sea Mapping oil spills Sea vessel detection Climate change monitoring
--

**Table 1.** Sentinel-1 main characteristics.

Sentinel-1 can produce 4 types of products:

- Level-0: is the Synthetic aperture radar (SAR) raw data.
- Level-1: there are two types of products in this class:
  - Single Look Complex (SLC): This product keeps their phase information, which is essential to perform the MT-InSAR technique.
  - Ground Range Detected (GRD): This product is processed so it loses their phase information. The GRD products can be in: Full Resolution (FR), High Resolution (HR) and Medium Resolution (MR).
- Level-2: focuses on the oceanic study of the earth's surface and includes the following components: Ocean Swell spectra, Ocean Wind Field and Surface Radial Velocity.

## 2. RELATED WORKS

### 2.1 Machine Learning predictive algorithms with MT-InSAR

The data generated through MT-InSAR can be used to perform predictive works through Machine Learning algorithms. Machine Learning is the branch of the field of artificial intelligence that seeks to provide machines with learning capacity, understood as the generalization of knowledge from a set of experiences. Based on the type of data output, there are 2 different types of algorithms in Machine Learning:

- Regression algorithms: used to predict the outcome of a trend.
- Classification algorithms: used to determine if a result belongs to one category or another.

There are numerous works that use information from radar images and the calculation of displacement on the earth's surface through MT-InSAR where different algorithms are used to predict the outcome of a trend (Regression algorithms), useful for the purpose of this research, some of them are: Linear Regression (L. Shi et al., 2020); Polynomial Regression (L. Shi et al., 2020); Support Vector Regression (Y. Shi et al., 2020); Random Forest Regression (Azarakhsh et al., 2022; Umarhadi et al., 2022). However, it is important to clarify that Machine Learning models can suffer the following prediction problems:

- Overgeneralization or underfitting occurs when a model is too simple and does not even fit the training data.
- Overfitting appears when a model is very complex and it fits the training examples well, but the

test examples poorly (it is not capable of to generalize).

## 2.2 State of the art in urban infrastructure monitoring using MT-InSAR

There are many cases of success in monitoring infrastructure in the city through the MT-InSAR technique and radar satellite images: Comparison of results in the detection of movements in the monitoring of the city of Urayasu, Japan between different satellites (from 1993 to 2006 with the ERS-1/-2 satellite (C band), from 2006 to 2010 with ALOS PALSAR (L band) and from 2014-2017 with the ALOS-2 PALSAR-2 (L-band)) through the SARscape program (Aimaiti et al., 2018); monitoring of damaged buildings in the city of Bratislava in 2014, through the SARPROZ program and the ENVISAT satellite (Bakon et al., 2014); monitoring of the urbanized sector of the municipalities of Portogruaro and Concordia Sagittaria, located in Italy with different satellites (ERS 1/2, ENVISAT, COSMO SKYMed and Sentinel-1) over time (1992 to 2017) through the SARscape program to define the mechanical behaviour of soil helping locate suitable areas for infrastructure (Floris et al., 2019).

Until now, there is no evidence of works that use satellite radar images and Machine Learning to perform predictive analysis specifically in collapsed urban infrastructures. The most similar works to this approach focus on a methodology for predicting and mapping surface motion beneath road pavement structures caused by environmental factors by Regression Tree, Support Vector Machine, Boosted Regression Trees and Random Forest (Fiorentini et al., 2020); Prediction of time-series deformation using deep convolutional neural networks (Ma et al., 2019); prediction through Influencing Factors the cumulative ground deformation using back-propagation (Wang et al., 2019); land deformation prediction by deep-learning (Radman et al., 2021).

In other words, all these approaches focus on predicting the displacement of certain study areas, but not on predicting collapses or studying cases where they have actually occurred.

Therefore, the present work wants to take the advantage of the predict capacity of Machine Learning regression algorithms in the anticipation of infrastructure collapses.

For this, the following methodology and case study are proposed: Prediction of the collapse of the pier, on August 12, 2018, during the O Marisquiño Festival in Vigo, using MT-InSAR and Machine Learning in order to set up a starting point in the investigation with the hope of building, together, in the future, more resilient cities in the face of the different challenges that may occur.

## 3. MATERIALS AND METHODS

### 3.1 Case Study

The analysis site is located in the city of Vigo (Galicia, Spain), with the aim of monitoring the displacements registered in the

Vigo pier at the O Marisquiño Festival prior to its collapse on August 12, 2018.

The collapse was in the surfside of Vigo (Figure 1), therefore, in a maritime environment. The infrastructures close to the sea are more exposed to deterioration due to environmental causes in comparison to other outside the coastal margins. There are many environmental causes of infrastructure deterioration like the exposure to the sea, the consequences of strong storms, salinity of the sea, etc. It is necessary to pay more attention on the part of the authorities in the monitoring of structural failures in them.

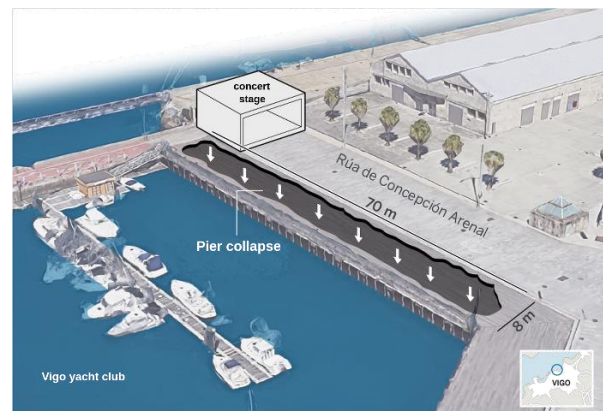


Figure 1. Situation of the collapsed pier.

Therefore, it is precise and pertinent, within the Smart City paradigm, to introduce MT-InSAR and Machine Learning as an additional monitoring technique, with the aim of knowing the state of infrastructures, preserving them, and avoiding catastrophes through alerts and emergency notification systems. This resilient vision is the maximum of the new urbanism, also called resilient urbanism (Sharifi & Yamagata, 2014).

### 3.2 Data Used

The predictive infrastructure monitoring through radar satellite images, MT-InSAR and Machine Learning begins with the download of 23 SLC type images (1 Master and 22 Slaves) of Sentinel-1 through the Alaska Satellite Facility Vertex download portal: <https://search.asf.alaska.edu/#/> (Figure 2).

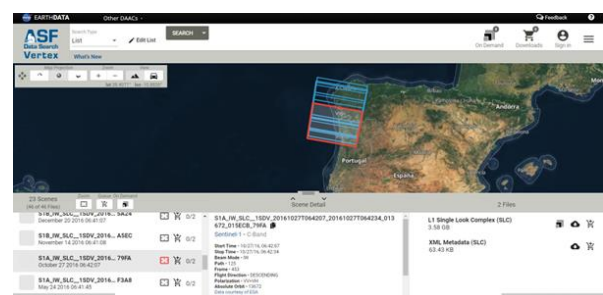


Figure 2. Selection for downloading 22 radar images as slaves (in blue) and 1 master radar image (in red).

The data was acquired (Table 2) with VV polarization, in descending orbit and operating in C-band (wavelength around 5.5 cm).

Master	27/10/2016
Slaves	from 01/12/2014 to 06/08/2018
Track	125
Bperp	max -74.71
Modeled Coherence	min 0.36

**Table 2.** Overview of the image stack and selection of the optimal MT-InSAR master image.

As the images are large, it is necessary to make a subset within SNAP program (<https://step.esa.int/main/download/snap-download/>) only for the study area (mainly the city of Vigo, and more specifically the pier that has suffered the collapse) (Figure 3).

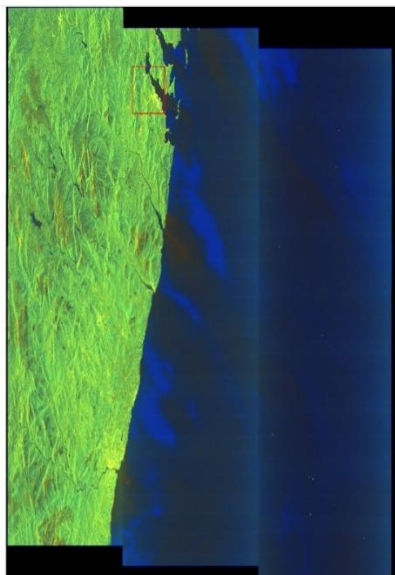


**Figure 3.** Full coverage of the master image downloaded for processing in SNAP. In the red box, the site of the city of Vigo, which will only be used as a study area in StaMPS program.

Depending on the path (ascending or descending) a different geometry is obtained (Figure 4). In this case, the master image is upside down because the image was acquired in descending orbit.

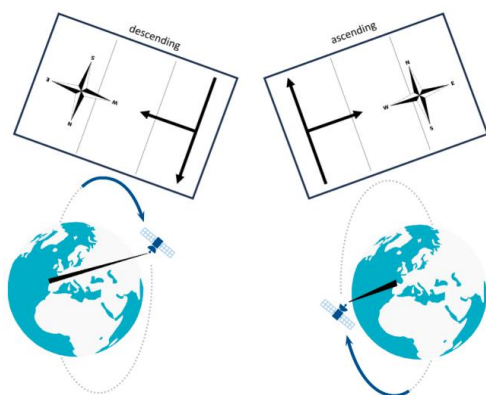


**Figure 4.** Difference between the capture geometry in the result of a descending orbit versus an ascending orbit.

### 3.3 Methods

The processing with the 23 images is based in MT-InSAR (Multi-Temporal Interferometry Synthetic Aperture Radar) technique by using the StaMPS program that can be downloaded from <http://homepages.see.leeds.ac.uk/~earahoo/stamps/> or <https://github.com/dbekaert/stamps>. The original development of StaMPS took place at Stanford University, but further evolution of StaMPS to StaMPS/MTI took place at the University of Iceland, Delft University of Technology, and the University of Leeds. Because it is an open-source program, there are also contributions made by the community.

The analysis with StaMPS starts with the selection of the master image and the co-registration of the rest of SLC (Level-1 Single Look Complex, this is a type of product that offers the Sentinel-1 satellite of radar images) slave images, so that they have the same geometry with the free ESA program SNAP (SNAP – STEP, n.d.). Once this is done by using snap2stamps (<https://github.com/mdelgadoblasco/snap2stamps>), which allows to automate the processing chain compatible with StaMPS (Blasco & Foumelis, 2018), the analysis begins with StaMPS, which provides the processing code to be executed with MATLAB (<https://www.mathworks.com/products/matlab.html>). This code consists of the series of instructions or steps to obtain information points with the displacements of the earth's surface (A. Hooper et al., 2012). In addition, for this work the following parameters (Table 3) related to the study of infrastructures are assigned:

Parameter	Default	Used
max_topo_err	20	10
filter_grid_size	50	40
clap_win	32	16
scla_deramp	'n'	'y'
percent_rand	20	1
unwrap_grid_size	200	50
unwrap_time_win	730	180
scn_time_win	365	180
scn_wavelength	100	50
unwrap_gold_n_win	32	16

**Table 3.** Parameters used for processing adjustment.

With the information points (PS or Permanent Scatterer), the displacement map of the study area is obtained. From here, the StaMPS-Visualizer program ([https://github.com/thho/StaMPS\\_Visualizer](https://github.com/thho/StaMPS_Visualizer)) (GitHub - Thho/StaMPS\_Visualizer: Shiny Application to Visualize DInSAR Results Processed by StaMPS/MTI, n.d.) is used for visualization.

Therefore, there are 3 stages in the workflow for data collection (PS):

- Interferogram processing using SNAP (1st stage). (For more details, consult the RUS Webinar at <https://www.youtube.com/watch?v=Xy7Y4Ea5mOo>).

- PS generation using StaMPS (2nd stage). (For more details, consult the StaMPS user manual at [https://homepages.see.leeds.ac.uk/~earahoo/stamps/StaMPS\\_Manual\\_v4.1b1.pdf](https://homepages.see.leeds.ac.uk/~earahoo/stamps/StaMPS_Manual_v4.1b1.pdf)).
- Analysis of results through StaMPS-Visualizer (3rd stage). (For more details, consult the StaMPS-Visualizer 3.0 Manual at [https://thho.shinyapps.io/StaMPS\\_Visualizer/](https://thho.shinyapps.io/StaMPS_Visualizer/)).

Once the PS are obtained, the predictive analysis is done with Machine Learning by the Python programming language in the Spyder environment. For this, the library that adds support in the realm of Machine Learning, Scikit-learn (<https://scikit-learn.org/stable/>) is used. It features several classification, regression, and clustering algorithms including support vector machines, random forests, gradient boosting, k-means, and DBSCAN, and is designed to interoperate with the Python scientific and numerical libraries NumPy and SciPy.

To do this, the data is restructured in a new file selecting just the PS of the collapse of the pier, so that it is easier to manipulate in Spyder: the accumulated speeds and their dates are selected (UNIX time format in days, this format is the StaMPS output format), each parameter in a column, and the average speed and the rest of PS are eliminated. Therefore, the features used for training are the displacement value registered for each of the PS throughout the analysis time.

In order to choose the most optimal models for the prediction of infrastructure collapses, a previous study is carried out based on the optimization of the model, comparing all the Regression algorithms evaluated in this work (Linear Regression, Polynomial Regression, Support Vector Regression and Random Forest Regression), the conclusion is the 2 most appropriate algorithms are:

- Support Vector Regression because its implementation is simple and it is suitable for small data sets.
- Random Forest Regression because it is very useful for applications where precision is very important.

The use of these 2 types of algorithms in this work enable to compare and better understand the results of the prediction.

In addition, for the 2 algorithms to be comparable, the automatically generated model must have an  $R^2$  above 0.80, and increase it as this value is reached, in order to be able to accurately predict the displacement the day of the collapse.

Finally, just with Support Vector Regression, a rescaling of the data must be done (so it is more difficult to interpret the data graphically, since the units are not the same as in the source).

#### 4. RESULTS AND VALIDATION

A mean displacement map is generated along the satellite's line of sight (LOS) through the velocity value of each of the Permanent Scatterers, the range of the displacement velocity values are  $-6$  mm/year to  $+6$  mm/year in the entire city of Vigo, the mean displacement map has the sufficient resolution to

detect deformations in infrastructures. The data set generates 80459 PS, so it is necessary to reduce the amount of information points, focusing only on the pier. The information points pier filtered are the PS 23, 24, 25, 26, 27, 28 and 29.

##### 4.1 Urban monitoring

The values of the mean displacement map (Figure 5) show that Vigo remains stable since in almost the entire city it does not present extreme values; In this sense, the stability of the Vigo area exposes the fact that most of the points are within  $\pm 2$  mm/year of displacement. However, a higher deformation rate is identified around the port and the pier with values that reach subsidence values of  $-3.5$  mm/year; This may be due to the influence exerted by the sea on the coast, so these infrastructures may be affected to a greater extent by global climate change.

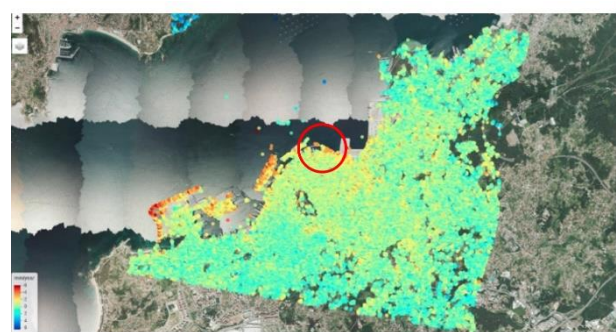


**Figure 5.** Displacement recorded in the study area with StaMPS and the location of the pier in red circle.

##### 4.2 Infrastructure monitoring

The PS 23, 24, 25, 26, 27, 28 and 29 show a clear trend of subsidence of the pier prior to the collapse (Figure 6).

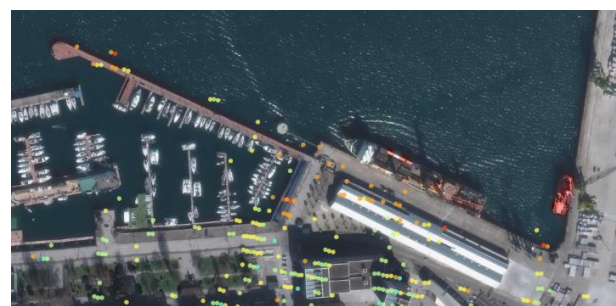


**Figure 6.** Details of the PS and their location in the Vigo Pier area.

A trend comparison graph is generated with the PS inside the pier (23, 24, 25, 26, 27, 28 and 29) (Figure 7).

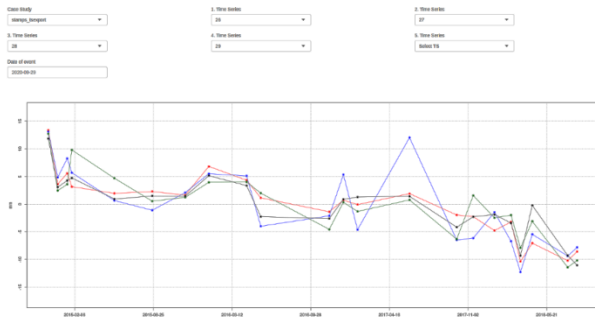


**Figure 7.** Relation between the PS obtained in the Pier and comparison over time before its collapse.

Before the pier collapse in the festival of O Marisquiño (August 12, 2018), the trend graph shows through the information points pier filtered (23, 24, 25, 26, 27, 28 and 29) a certain homogeneous subsidence trend, because on the dates of the analysis the evolution of the displacement passes approximately from +12 mm in the first shot (01/12/2014) to -5 mm in the last shot (06/08/2018) before the collapse.

### 4.3 Predicting infrastructure displacement

Although 23 images are enough to obtain results with the MT-InSAR technique, it seems insufficient to be able to obtain consistent results for long future prediction projections, however for technical storage problems (it must be remembered that the MT-InSAR process is computationally excessively expensive due to the weight of the images), it is decided to carry out an analysis capable of containing a long analysis period but reducing the number of satellite images to optimize the best possible computational resources available. The lack of a huge set of data makes the use of deep learning unfeasible, so classic machine learning techniques are chosen that are capable of giving predictions with less data.

To carry out the predictive analysis, 60% of the PS of the pier are selected, prior to the collapse, and the remaining 40% of the PS is used as validation.

For training with Support Vector Regression of 60% of the data (Figure 8), the value obtained as a prediction for the day of the collapse (August 12, 2018) is -10.02745702 mm/year, with a model precision of 0.8664182342003215.

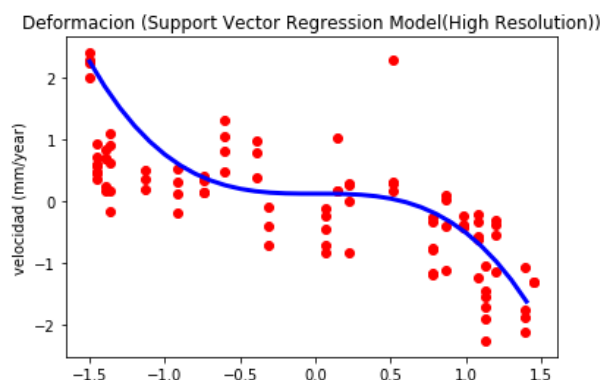


**Figure 8.** Training values and the generated model, Support Vector Regression.

For training with Random Forest Regression of 60% of the data (Figure 9), the value obtained as a prediction for the day of the collapse (August 12, 2018) is -8.87695843 mm/year, with a model precision of 0.9019062465302864.

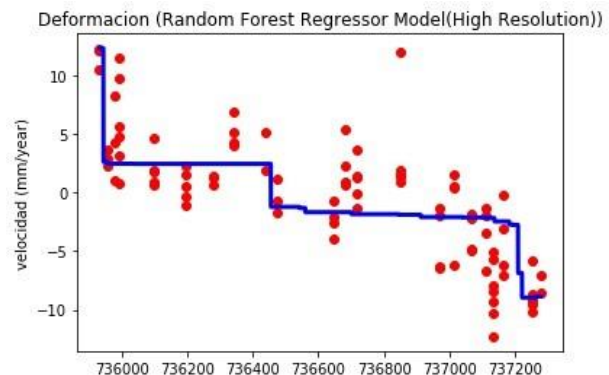


**Figure 9.** Training values and the generated model, Random Forest Regression.

Both generated models show a displacement value greater than 8.8 mm/year (considered an extreme value) obtained for the day the pier collapsed. Likewise, since May 28, 2018, the registered displacements are above -5mm/year, which is already considered an extreme displacement. So, it is shown that the high rate of displacement speed for that day was predictable.

### 4.4 Validation

To check the accuracy of the results obtained by MT-InSAR, a comparison is made with the LIDAR (Laser Imaging Detection and Ranging) information available in the CNIG Download Web:

<http://centrodedescargas.cnig.es/CentroDescargas/buscadorCatalogo.do?codFamilia=LIDAR>. The choice of LIDAR data responds to its free availability and its great spatial coverage, it also offers a high density of points, so it can reconstruct the surfaces and infrastructures of study, this makes it possible to measure the height of objects and as it varies over the years.

For this purpose, the only existing data to date are used: LIDAR PNOA from 2011 (1st coverage) and 2015 (2nd coverage). In this situation, only LIDAR data from 2015 can be compared with Sentinel-1 data, since Sentinel-1 only begins to have data from 2014 and the analysis begins by the end of 2014.

The error analysis is only carried out for the data that coincide in dates and location, for which a projection is made, in both data sets, to obtain the "theoretical" rates of deformation in the same period (2014-2015).

Most of the coincident pixels between the two data sources show an error close to zero (Figure 10), so the MT-InSAR technique is validated as a useful and reliable tool for infrastructure monitoring.

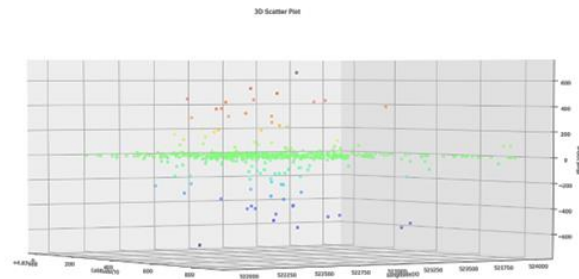


**Figure 10.** Error value of the coincident pixels between the two data sources, with their UTM coordinates (WGS84 / UTM zone 28N).

The final result of the analysis shows that this type of monitoring is appropriate for infrastructure control since it produces a series of points with millimetre resolution. If there is subsidence, the recorded values will be negative, and positive if there is uplift. In addition, if it presents non-stable values (above +2 mm/year and below -2 mm/year), it is necessary to carry out a timely monitoring of the infrastructure affected by these values. It must be remembered that these values are always referred to the line of sight of the satellite (LOS) to the ground and not to the vertical or horizontal displacement ( $\Delta Z$ ) (Figure 11).

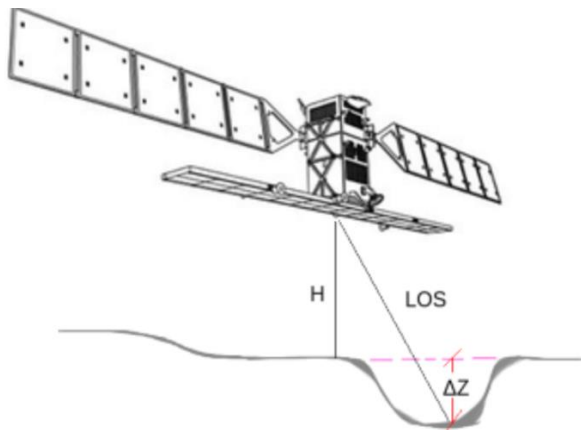


**Figure 11.** Relation between LOS and vertical displacement ( $\Delta Z$ ).

## 5. CONCLUSIONS

The present work exhibits monitoring urban infrastructures, without large material costs, effectively and with consistent results by radar satellite images (Sentinel-1). In this sense, the use of Machine Learning represents a true revolution for disaster prediction and its use as a predictor of future infrastructure locations, being an ideal complement for decision-making for urban authorities. This predictive monitoring capable of anticipating risks is one of the objectives of the new urbanism focus on the resilience.

It should be noted that, with the use of MT-InSAR millimetric displacements can be detected, but this does not mean that the results are the same as those obtained with other techniques such as the use of GPS, mobile mapping, etc. Because all the movements detected with MT-InSAR are relative, that is, the movement detected is referred to the satellite, so it is hard to make a comparison in terms of recording the same values, with other monitoring techniques. The comparison between

techniques, therefore, allows to validate whether or not there is movement in the area, but does not allow the verification of whether the value of the displacement coincides.

Therefore, this work achieved the detection of where the movements are located and if they are candidates for a more detailed study. Finally, this work supposes the confirmation of the use of radar satellite images, MT-InSAR and Machine Learning as a monitoring complement on infrastructures in the city as a model of good practices and to achieve a Smart City. This work shows the workflow for the prediction and location of extreme events.

However, to obtain a much more robust analysis, it is important to carry out an analysis with a greater number of images that allow reducing the uncertainties in the results through Machine Learning. In this sense, the comparison with other works that use deep learning techniques is less computationally expensive but contains more uncertainties in its results, if it is compared with works where classic machine learning techniques are used, this work has the advantage of only using displacement information, without the need to create new layers of information that it is not possible to obtain in all geographical areas.

## ACKNOWLEDGEMENTS

Work produced with the support of a 2021 Leonardo Grant for Researchers and Cultural Creators, BBVA Foundation. The BBVA Foundation takes no responsibility for the opinions, statements and contents of this project, which are entirely the responsibility of its authors.

## REFERENCES

- Aimaiti, Y., Yamazaki, F., & Liu, W. (2018). Multi-sensor InSAR analysis of progressive land subsidence over the coastal city of Urayasu, Japan. *Remote Sensing*, 10(8), 1304. <https://doi.org/10.3390/RS10081304>
- Anthopoulos, L. (2015). Understanding the Smart City Domain: A Literature Review. In: Rodríguez-Bolívar, M. (eds) *Transforming City Governments for Successful Smart Cities*. Public Administration and Information Technology, vol 8. Springer, Cham. [https://doi.org/10.1007/978-3-319-03167-5\\_2](https://doi.org/10.1007/978-3-319-03167-5_2)
- Azaraksh, Z., Azadbakht, M., & Matkan, A. (2022). Estimation, modeling, and prediction of land subsidence using Sentinel-1 time series in Tehran-Shahriar plain: A machine learning-based investigation. *Remote Sensing Applications: Society and Environment*, 25. <https://doi.org/10.1016/J.RSASE.2021.100691>
- Bakon, M., Perissin, D., Lazecky, M., & Papco, J. (2014). Infrastructure Non-linear Deformation Monitoring Via Satellite Radar Interferometry. *Procedia Technology*, 16, 294–300. <https://doi.org/10.1016/J.PROTCY.2014.10.095>
- Blasco, J. M. D., & Foumelis, M. (2018). Automated SNAP Sentinel-1 DInSAR processing for StaMPS PSI with open source tools. <https://doi.org/10.5281/ZENODO.1322353>
- Cian, F., Blasco, J., & Carrera, L. (2019). Sentinel-1 for Monitoring Land Subsidence of Coastal Cities in Africa Using PSInSAR: A Methodology Based on the Integration of SNAP

- and StaMPS. *Geosciences*, 9(3), 124. <https://doi.org/10.3390/geosciences9030124>
- Crosetto, M., Monserrat, O., Cuevas-González, M., Devanthery, N., & Crippa, B. (2016). Persistent Scatterer Interferometry: A review. *ISPRS Journal of Photogrammetry and Remote Sensing*, 115, 78–89. <https://doi.org/10.1016/J.ISPRSJPRS.2015.10.011>
- Fiorentini, N., Maboudi, M., Leandri, P., Losa, M., & Gerke, M. (2020). Surface motion prediction and mapping for road infrastructures management by PS-InSAR measurements and machine learning algorithms. *Remote Sensing*, 12(23), 1–60. <https://doi.org/10.3390/rs12233976>
- Floris, M., Fontana, A., Tessari, G., & Mulè, M. (2019). Subsidence Zonation Through Satellite Interferometry in Coastal Plain Environments of NE Italy: A Possible Tool for Geological and Geomorphological Mapping in Urban Areas. *Remote Sensing*, 11(2), 165. <https://doi.org/10.3390/rs11020165>
- GitHub - thho/StaMPS\_Visualizer: Shiny application to visualize DInSAR results processed by StaMPS/MTI. (n.d.). Retrieved January 4, 2021, from [https://github.com/thho/StaMPS\\_Visualizer](https://github.com/thho/StaMPS_Visualizer)
- González, P. (2010). Medida y caracterización de deformaciones usando técnicas geodésicas y de teledetección. Aplicación en volcanología y sismotectónica. técnicas geodésicas y de teledetección.
- Hooper, A., Bekaert, D., Spaans, K., & Arikan, M. (2012). Recent advances in SAR interferometry time series analysis for measuring crustal deformation. *Tectonophysics*, 514–517, 1–13. <https://doi.org/10.1016/J.TECTO.2011.10.013>
- Hooper, A. J. (2008). A multi-temporal InSAR method incorporating both persistent scatterer and small baseline approaches. *Geophysical Research Letters*, 35(16). <https://doi.org/10.1029/2008GL034654>
- Juan Gabriel Arroyo Parras, & Antonio Miguel Ruiz Armenteros. (2017). Monitorización de la deformación del terreno de la metrópolis de Warri (Nigeria), por medio de la técnica Multi-temporal de Interferometría Radar de Apertura Sintética (MT-InSAR). [Universidad de Jaén]. <http://tauja.ujaen.es/handle/10953.1/6077>
- Ma, P., Zhang, F., & Lin, H. (2019). Prediction of InSAR time-series deformation using deep convolutional neural networks. *Remote Sensing Letters*, 11(2), 137–145. <https://doi.org/10.1080/2150704X.2019.1692390>
- Radman, A., Akhoondzadeh, M., & Hosseiny, B. (2021). Integrating InSAR and deep-learning for modeling and predicting subsidence over the adjacent area of Lake Urmia, Iran. *GIScience & Remote Sensing*, 58(8), 1413–1433. <https://doi.org/10.1080/15481603.2021.1991689>
- Sharifi, A., & Yamagata, Y. (2014). Resilient Urban Planning: Major Principles and Criteria. *Energy Procedia*, 61, 1491–1495. <https://doi.org/10.1016/j.egypro.2014.12.154>
- Shi, L., Gong, H., Chen, B., & Zhou, C. (2020). Land Subsidence Prediction Induced by Multiple Factors Using Machine Learning Method. *Remote Sensing*, 12(24), 4044. <https://doi.org/10.3390/rs12244044>
- Shi, Y., Li, Q., Meng, X., Zhang, T., & Shi, J. (2020). On Time-Series InSAR by SA-SVR Algorithm: Prediction and analysis of mining subsidence. *Journal of Sensors*. <https://doi.org/10.1155/2020/8860225>
- SNAP – STEP. (n.d.). Retrieved January 3, 2022, from <http://step.esa.int/main/toolboxes/snap/>
- Umarhadi, D. A., Widyatmanti, W., Kumar, P., Yunus, A. P., Khedher, K. M., Kharrazi, A., & Avtar, R. (2022). Tropical peat subsidence rates are related to decadal LULC changes: Insights from InSAR analysis. *Science of the Total Environment*, 816. <https://doi.org/10.1016/J.SCITOTENV.2021.151561>
- Wang, Y., Guo, Y., Hu, S., Li, Y., Wang, J., Liu, X., & Wang, L. (2019). Ground Deformation Analysis Using InSAR and Backpropagation Prediction with Influencing Factors in Erhai Region, China. *Sustainability*, 11(10), 2853. <https://doi.org/10.3390/su11102853>
- Xue, F., Lv, X., Dou, F., & Yun, Y. (2020). A Review of Time-Series Interferometric SAR Techniques: A Tutorial for Surface Deformation Analysis. *IEEE Geoscience and Remote Sensing Magazine*, 8(1), 22–42. <https://doi.org/10.1109/MGRS.2019.2956165>